IL NUOVO CIMENTO Vol. 36 C, N. 6 Novembre-Dicembre 2013
DOI 10.1393/ncc/i2014-11645-2

Colloquia: LaThuile13

Recent Higgs $\to ZZ^{(*)} \to 4l$ results with the ATLAS experiment

A. Salvucci on behalf of the ATLAS Collaboration

Radboud University Nijmegen - Nijmegen, The Netherlands and Nikhef, Amsterdam, The Netherlands

ricevuto 20 Giugno 2013; approvato l'1 Luglio 2013

Summary. — This document presents a short update of the search results and a first measurement of the properties of the newly observed Higgs-like particle in the decay channel $H \to ZZ^{(*)} \to l^+l^-l'^+l'^-$, where $l, l' = e$ or μ, using $4.6\,\text{fb}^{-1}$ and $13\,\text{fb}^{-1}$ of proton-proton collisions at $\sqrt{s} = 7$ and $\sqrt{s} = 8\,\text{TeV}$, respectively, recorded with the ATLAS detector at the LHC. An excess of events over background is seen, with a minimum p_0 value of 0.0021% (4.1 standard deviations) at $m_H = 123.5\,\text{GeV}$ in the combined analysis of the two datasets. The fitted Higgs mass is measured to be $m_H = 123.5 \pm 0.9$ (stat.) ± 0.3 (syst.) GeV and the signal strength (the ratio of the observed cross-section to the expected SM cross-section) at this mass is found to be $\mu = 1.3^{+0.5}_{-0.3}$. A spin-parity analysis is performed on the events with $115\,\text{GeV} < m_H < 130\,\text{GeV}$. The 0^+ state is found to be favoured over the 0^- and 2^+ states with 0^- excluded by 2.7 σ when compared to 0^+.

PACS 14.80.Bn – Standard-model Higgs boson.

1. – Introduction

Recently the ATLAS and CMS experiments have reported the observation of a new particle in the search for the Standard Model Higgs Boson [1, 2], where one of the most sensitive channels is $H \to ZZ^{(*)} \to 4l$. An important step in the confirmation of the new particle as the SM Higgs boson is the measurement of its spin and parity J^P, predicted to be 0^+.

The search of the SM Higgs boson through the decay $H \to ZZ^{(*)} \to 4l$, where $l = e$ or μ, provides good sensitivity over a wide mass range. Four distinct final states, 4μ, 4e, 2μ2e and 2e2μ are selected. The 2μ2e and 2e2μ differ by the flavor of the lepton pair closest to the Z mass. The largest background in this search comes from continuum $(Z^{(*)}/\gamma^*)(Z^{(*)}/\gamma^*)$ production, referred as $ZZ^{(*)}$ hereafter. For masses below 160 GeV, there are also important background contributions from Z+jets and $t\bar{t}$ production, where the additional charged lepton candidates arise either from decays of hadrons with b- or c-quark content or from mis-identification of jets.

This documents is a quick summary of results presented in December 2012 [3]. It includes the analysis of $\sqrt{s} = 7\,\text{TeV}$ data, corresponding to an integrated luminosity of $4.6\,\text{fb}^{-1}$ collected in 2011, combined with the analysis of $\sqrt{s} = 8\,\text{TeV}$ data, corresponding to an integrated luminosity of $13\,\text{fb}^{-1}$ collected between April and September 2012. The analysis concentrates on the spin and parity (J^P) of the $H \to ZZ^{(*)} \to 4l$ decay to distinguish between the states with spin 0 and 2, even and odd parity, through the obseved distributions of the two Z boson masses, one production and four decay angles.

2. – Event selection and backgrounds

The data are subjected to quality requirements: events recorded during periods when the relevant detector components were not operating normally are rejected. These requirements are applied independently of the lepton final state.

2˙1. *Event selection.* – The data considered in this analysis are selected using single-lepton or di-lepton triggers [3]. This analysis searches for Higgs boson candidates by selecting two same-flavour, opposite-sign lepton pairs in an event. Each electron (muon) must satisfy $E_T > 7\,\text{GeV}$ ($p_T > 6\,\text{GeV}$) and be measured in the pseudo-rapidity range $|\eta| < 2.47$ ($|\eta| < 2.7$). The first three leptons composing the quadruplet must satisfy the p_T requirement of 20, 15 and 10 GeV. The leptons are required to be separated from each other by $\Delta R > 0.1$ (0.2) if they are of the same flavour (otherwise). The same-flavour and opposite-sign lepton pair closest to the Z boson mass is referred to as the leading di-lepton and its invariant mass, m_{12}, is required to be between 50 and 106 GeV. The remaining same-flavour, opposite-sign lepton pair is the sub-leading di-lepton and its invariant mass, m_{34}, is required to be in the range $m_{min} < m_{34} < 115\,\text{GeV}$, where m_{min} depends on the reconstructed four-lepton invariant mass, m_{4l}, and varies from 17.5 to 50 GeV. The Z boson corresponding to the leading (sub-leading) di-lepton pair is labelled Z_1 (Z_2). All possible same-flavour opposite-charge di-lepton combinations in the quadruplet must satisfy $m_{ll} > 5\,\text{GeV}$ to remove events containing $J/\Psi \to ll$. To all leptons isolation cuts are also applied: each lepton is required to have a normalised track isolation smaller than 0.15, while the normalized calorimetric isolation has to be smaller than 0.20 (0.30) for electrons (muons). Finally, the impact parameter significance, defined as the impact parameter divided by its uncertainty, d_0/σ_{d_0}, for all muons (electrons) is required to be lower than 3.5 (6.5).

2˙2. *Background estimation.* – The level of the irreducible $ZZ^{(*)}$ background is estimated using MC simulation normalised to the theoretical cross section, while the rate and composition of the reducible Z+jets and $t\bar{t}$ background processes are evaluated with data-driven methods. The composition of the reducible backgrounds depends on the flavour of the sub-leading di-lepton and different approaches are taken for the $ll+\mu\mu$ and the $ll+ee$ final states. This is done in order to estimate the yields of the reducible background and estimate the correct normalization through a data driver technique (fig. 1). The $ll + \mu\mu$ reducible background arises from $t\bar{t}$ and $Z+$jets. The number of background events from $t\bar{t}$ and $Z +$ jets is estimated from two control regions: one with an enhanced $b\bar{b}$ contribution and π/K in-flight decays and the other with both components augmented. An $ll + ee$ background control region is formed by relaxing the electron selection criteria for the electrons of the sub-leading pair. The shape and normalisation of the backgrounds are in good agreement with data.

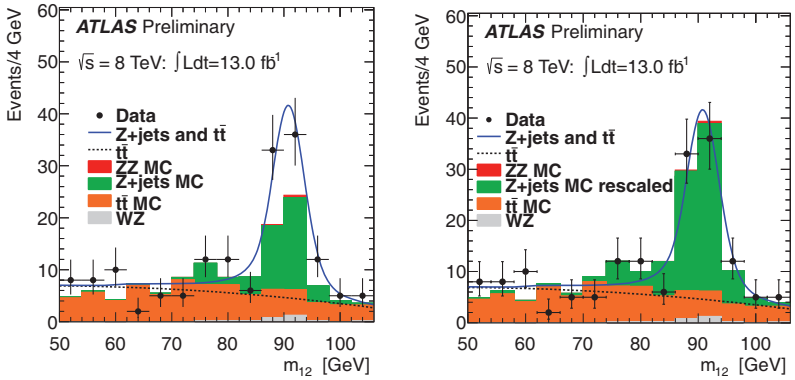

(a) (b)

Fig. 1. – Distribution of m_{12}, for $\sqrt{s} = 8\,\text{TeV}$, in the control region where the isolation requirements are not applied to the two sub-leading muons. (a) Fit used to obtain the yields for $t\bar{t}$ and Z + jets; (b) same distribution with the Z + jets MC rescaled by the data fit [3].

3. – Spin and parity measurement

For $X \to ZZ^{(*)} \to 4l$ decays, the observables sensitive to the underlying spin and parity of X are the masses of the two Z bosons, a production angle, θ^*, and four decay angles, Φ_1, Φ, θ_1 and θ_2. The production and decay angles are illustrated in fig. 2 and are defined as

- θ_1 (θ_2) is the angle between the negative final state lepton and the direction of flight of Z_1 (Z_2) in the Z rest frame.
- Φ is the angle between the decay planes of the four final state leptons expressed in the four lepton rest frame.
- Φ_1 is the angle defined between the decay plane of the leading lepton pair and a plane defined by the vector of the Z_1 in the four lepton rest frame and the positive direction of the parton axis.
- θ^* is the production angle of the Z_1 defined in the four lepton rest frame.

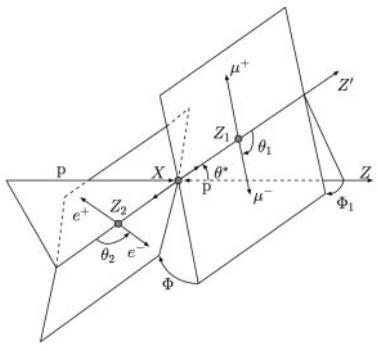

Fig. 2. – Definition of the production and decay angles in an $X \to ZZ^{(*)} \to 4l$. The illustration is drawn with the beam axis in the lab frame, the Z_1 and Z_2 in the X rest frame and the leptons in their corresponding parent rest frame [3].

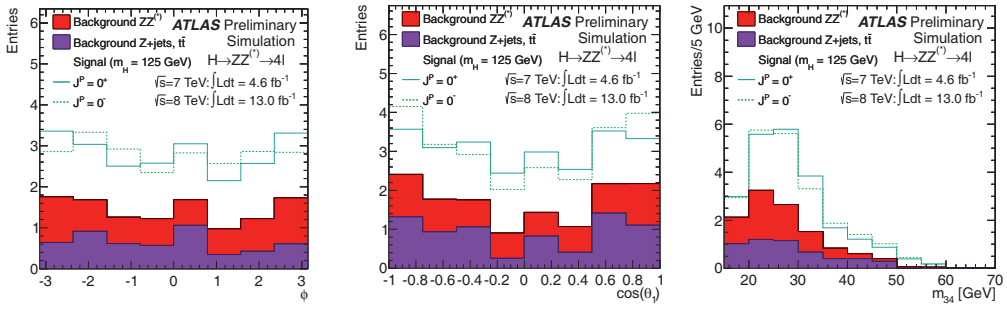

(a) (b) (c)

Fig. 3. – Expected distributions for $\sqrt{s} = 7$ and $\sqrt{s} = 8\,\text{TeV}$ for $m_H = 125\,\text{GeV}$ including backgrounds in the mass range $115 < m_{4l} < 130\,\text{GeV}$ comparing two pairs of spin/parity J^P states. Comparison of 0^+ *versus* 0^- hypotheses: (a) Φ, (b) $\cos\theta_1$, and (c) m_{34} [3].

Two approaches have been pursued to develop the discriminants used to distinguish between the pairs of spin/parity states. One uses a boosted decision tree (BDT) in a multivariate analysis. The other uses the theoretical differential decay rate for the angles, m_{12} and m_{34}, corrected for detector acceptance and analysis selection, to construct a matrix-element–based likelihood ratio (MELA) [4] as a discriminant between the different spin-parity hypotheses. For the BDT approach, a J^P discriminant is formed for each pair of spin/parity states to be tested by training a BDT on the variables of fully simulated signal events which fall in the mass window $115 < m_{4l} < 130\,\text{GeV}$. This is done for all four-lepton final states combined. For the backgrounds, the rates and the m_{4l} shapes are taken from the analyses described in sect. **2**. The response of the J^P discriminants is evaluated for each background of the four final states and for each of the two mass bins. This BDT response is then added to the statistics model used in the profile likelihood fit, described below.

For the MELA approach, the probability for a particular spin/parity state can be calculated exactly for each event. This probability is corrected for detector acceptance and analysis selection which are obtained from the fully simulated JHU [5] signal MC samples. The full PDF also takes into account the incorrect pairing of the leptons for the 4μ and $4e$ channels, at the level of $\sim 20\%$ of events for spin 0, but has a negligible effect on the discrimination. For a pair of spin/parity states, a J^P discriminant is formed, labelled J^P-MELA from the ratio of this combined PDF for one of the spin/parity states to the sum of PDFs for both spin/parity states.

Candidate events in the region $115 < m_{4l} < 130\,\text{GeV}$ are used. Figure 3 shows the expected distributions of some J^P sensitive observables. To improve the overall sensitivity, this mass region is split into two bins of high and low signal over background (S/B): low (115–121 and 127–130 GeV), and high (121–127) GeV. The statistical test for a pair of spin/parity hypotheses, H_0 and H_1, uses the following probability model:

$$\mathcal{P}^{ij} = \mu^{sig} f_i^{sig} N_{sig} \left[(1-\varepsilon) \cdot PDF^{ij}_{H_0} + \varepsilon \cdot PDF^{ij}_{H_1} \right] + \sum_{bkg_k} f_i^{bkg_k} N_{bkg_k} PDF^{ij}_{bkg_k}, \tag{1a}$$

where μ^{sig} is the signal strength, N_{sig} is the number of signal events in the full mass region $115 < m_{4l} < 130\,\text{GeV}$, f_i^{sig} is the signal fraction in the i-th S/B mass bin (low and

TABLE I. – *The numbers of expected signal and background events together with the number of observed events, in a window of* ± 5 GeV *around* 125 GeV *for the combination of* 2011 *and* 2012 *data.*

$\sqrt{s} = 7$ and $\sqrt{s} = 8$ TeV				
	Signal ($m_H = 125$ GeV)	$ZZ^{(*)}$	$Z +$ jets, $t\bar{t}$	Observed
4μ	4.0 ± 0.5	2.03 ± 0.09	0.36 ± 0.09	8
$2\mu 2e$	1.7 ± 0.2	0.70 ± 0.05	1.21 ± 0.18	2
$2e2\mu$	2.4 ± 0.3	1.02 ± 0.05	0.30 ± 0.07	4
$4e$	1.8 ± 0.3	0.94 ± 0.09	1.72 ± 0.23	4
total	9.9 ± 1.3	4.7 ± 0.3	3.6 ± 0.3	18

high), and $(1-\varepsilon)$ is the fraction of the H_0 signal hypothesis represented by the $PDF^{ij}_{H_0}$ for the j-th J^P discriminant. Similarly, $f_i^{bkg_k}$, N_{bkg_k} and $PDF^{ij}_{bkg_k}$ are the bin fraction, total background and PDF for the k-th background, respectively. The parameters N_{sig}, N_{bkg_k} are nuisance parameters which are constrained by Gaussian terms, and their uncertainties are determined from the nominal analysis. The fractions of events in each of the two mass bins are constrained to sum to unity. The parameter μ^{sig} is left free in the fit.

4. – Results

4˙1. *Search result.* – Table I reports the observed and expected events, in a mass window of ± 5 GeV around a 125 GeV hypothesized Higgs Boson mass, for the combination of 2011 and 2012 data sets.

The expected m_{4l} distributions for the total background and one signal hypothesis are compared to the combined $\sqrt{s} = 7$ and $\sqrt{s} = 8$ TeV in fig. 4, for the low mass range 80–250 GeV. The effect on the reconstructed invariant mass due to photon emission from final state radiation (FSR) is modeled by the MC. High-p_T photon emission, occurring at

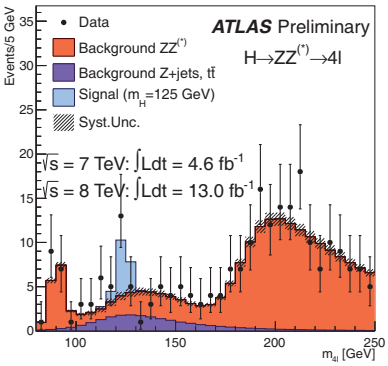

Fig. 4. – The distribution of the four-lepton invariant mass, m_{4l}, for the selected candidates compared to the background expectation for the combined $\sqrt{s} = 7$ and $\sqrt{s} = 8$ TeV data sets in the low mass range of 80–250 GeV. The signal expectation for the $m_H = 125$ GeV hypothesis is also shown [3].

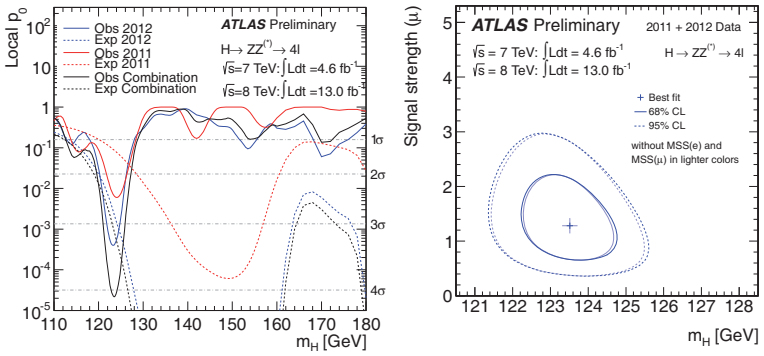

(a) (b)

Fig. 5. – (a) The observed p_0 for the combination of the 2011 and 2012 data sets (solid black line); the $\sqrt{s} = 7$ and $\sqrt{s} = 8\,\text{TeV}$ data results are shown in solid lines (blue and red, respectively). The dashed curves show the expected median local p_0 for the signal hypothesis when tested at the corresponding m_H. The horizontal dashed lines indicate the p_0 values corresponding to local significances of 1σ, 2σ, 3σ and 4σ. (b) Likelihood ratio contours in the μ, m_H plane that, in the asymptotic limit, correspond to 68% and 95% confidence level contours, shown with (dark color) and without (lighter color) MSS(e) and MSS(μ) [3].

a low rate, is not taken into account explicitly in the lepton reconstruction. All candidates in the selected mass window $120 < m_{4l} < 130\,\text{GeV}$ have been checked and no FSR-like photons were found with $E_T > 3.5\,\text{GeV}$. The significance of an excess is given by the probability p_0 that a background-only experiment is more signal-like in terms of the test statistic than the observed data. In fig. 5(a) the local p_0 is presented as a function of m_H hypothesys for $\sqrt{s} = 7\,\text{TeV}$, $\sqrt{s} = 8\,\text{TeV}$ and the combination. The global signal strenght factot μ acts as a scale factor on the total number of events predicted by the SM for each of the Higgs Boson signal processes. Figure 5(b) presents the best μ and m_H fit values and the profile likelihood ratio contours that, in the asymptotic limit, would correspond to 68% and 95% confidence level, shown with (dark dashed curve) the mass

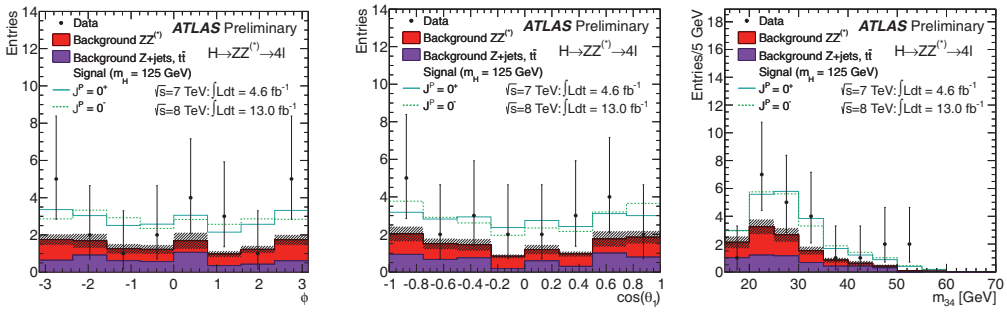

(a) (b) (c)

Fig. 6. – Distributions of some of the spin and parity sensitive observables for events passing the full selection in the signal mass window $115 \leq m_{4l} \leq 130\,\text{GeV}$ for the combined $\sqrt{s} = 7$ and $\sqrt{s} = 8\,\text{TeV}$ data sets. The expected contributions from the Higgs signal, irreducible $ZZ^{(*)}$ background as well as the measured contribution from reducible non-$ZZ^{(*)}$ backgrounds are shown. (a) Φ_1, (b) $\cos\theta_1$, (c) m_{34} [3].

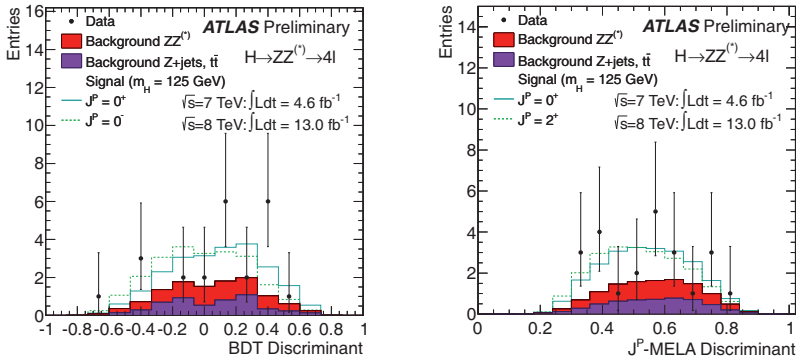

(a) (b)

Fig. 7. – Examples of distributions of the BDT and J^P-MELA discriminants for data and Monte Carlo expectations for the combined $\sqrt{s} = 7$ and $\sqrt{s} = 8$ TeV data sets. Panel (a) shows the 0^+ *versus* 0^- hypothesis for the BDT analysis; panel (b) shows the 0^+ *versus* 2^+_m for the J^P-MELA analysis [3].

scale systematics from electrons (MMS(e)) and muons (MSS(μ)) and without (lighter dashed curve). The value of the signal strength μ at the best fit for m_H (123.5 GeV) is $1.3^{+0.5}_{-0.4}$, while the value of the fitted mass is $m_H = 123.5 \pm 0.9$ (stat.) ± 0.3 (syst.) GeV.

4·2. *Spin and parity.* – Figure 6 shows the comparison of some spin and parity sensitive observables for events passing the full selection in the signal mass window $115 \leq m_{4l} \leq 130$ GeV, compared with the expected contributions from Higgs signal and backgrounds. Some distributions for the BDT and J^P-MELA discriminants are presented in fig. 7 comparing the J^P 0^+ hypothesis with the 0^- and 2^+ hypotheses. The discrimination between the different hypotheses has been studied using MC pseudo-experiments.

TABLE II. – *For an assumed* 0^+ *hypothesis* H_0*, the values for the expected and observed* p_0*-values of the different tested spin and parity hypotheses* H_1 *for the BDT and* J^P*-MELA analyses. The results are given combining* $\sqrt{s} = 7$ *and* $\sqrt{s} = 8$ TeV*. The* p_0*-value is also given in terms of the corresponding number of Gaussian* σ*. The observed* p_0*-value is also given for the* 0^+ *assumed hypothesis. Negative* σ *corresponds to* p_0*-values greater than* 0.5*.*

Tested J^P hypotheses for an assumed 0^+						
	0^-			2^+_m		
	expected	observed	obs 0^+	expected	observed	obs 0^+
BDT analysis						
p_0-value	0.041	0.011	0.69	0.20	0.16	0.57
σ	1.7	2.3	−0.50	0.84	0.99	−0.18
J^P-MELA analysis						
p_0-value	0.031	0.0028	0.76	0.18	0.17	0.53
σ	1.9	2.7	−0.72	0.91	0.97	−0.08

The expected and observed p_0-values when assuming the spin 0^+ hypothesis and testing the 0^- and 2^+_m are presented in table II. It can be observed that the Standard Model 0^+ hypothesis is preferred over the 0^- and 2^+_m hypotheses. All hypotheses are preferred over the 0^- hypothesis. Both the BDT and J^P-MELA approaches show similar exclusions. The results of these two different analyses both support the conclusion that the SM expectation of $J^P = 0^+$ is clearly preferred. The alternative spin and parity hypotheses are excluded with the following confidence levels for the BDT (J^P-MELA) analysis: 98.9% (99.7%) for 0^-, 84% (83%) for 2^+_m.

5. – Conclusions

Updated search results for the newly observed Higgs-like particle have been presented, using $4.6\,\text{fb}^{-1}$ of data at $\sqrt{s} = 7\,\text{TeV}$ and $13\,\text{fb}^{-1}$ at $\sqrt{s} = 8\,\text{TeV}$ recorded by the ATLAS detector. An excess of events above background is seen with the smallest p_0 of 0.0021% (4.1 standard deviations) at $m_H = 123.5\,\text{GeV}$.

The fitted mass is $123.5 \pm 0.9\,(\text{stat.}) \pm 0.3\,(\text{syst.})\,\text{GeV}$, and the signal strength of the Higgs-like particle at this mass is found to be $1.3^{+0.5}_{-0.4}$.

A first analysis of the spin and parity of the new particle has been presented. Hypothesis tests comparing the SM 0^+ J^P hypothesis with 0^-, 2^+_m have been performed. The SM spin and parity remain the favoured hypothesis, with the other spin parity hypotheses excluded at the following level using a BDT (J^P-MELA) analysis: 98.9% (99.7%) for 0^-, 84% (83%) for 2^+_m. In addition, the 0^- hypothesis is excluded when tested against the 2^+_m hypothesys with $p0$-values for BDT (J^P-MELA) of 99.85% (99.0%).

REFERENCES

[1] ATLAS Collaboration, *Phys. Lett. B*, **716** (2012) 1.
[2] CMS Collaboration, *Phys. Lett. B*, **716** (2012) 30.
[3] ATLAS Collaboration, *Updated results and measurements of properties of the new Higgs-like particle in the four lepton decay channel with the ATLAS detector*, ATLAS-CONF, 2012-169 (2012) `https://cds.cern.ch/record/1499628`.
[4] Bolognesi S. *et al.*, *Phys. Rev. D*, **86** (2012) 21.
[5] Gao Y. *et al.*, *Phys. Rev. D*, **81** (2010) 075022, arXiv:1001.3396 [hep-ph].